

High-Pressure Studies of $(\text{Mg}_{0.9}\text{Fe}_{0.1})_2\text{SiO}_4$ Olivine Using Raman Spectroscopy, X-ray Diffraction, and Mössbauer SpectroscopyJ. Rouquette,^{*,†,§} I. Kantor,[†] C. A. McCammon,[†] V. Dmitriev,[‡] and L. S. Dubrovinsky[†]*Bayerisches Geoinstitut, Universität Bayreuth, D-95440 Bayreuth, Germany, and European Radiation Synchrotron Facility (ESRF), Swiss-Norwegian Beam Lines (SNBL), BP220 38047 Grenoble CEDEX 9, France*

Received October 8, 2007

High-pressure studies of $(\text{Mg}_{0.9}\text{Fe}_{0.1})_2\text{SiO}_4$ olivine were performed at ambient temperature using X-ray diffraction, Raman spectroscopy, and Mössbauer spectroscopy. At ~ 40 GPa, a change of compressibility associated with saturation of the anisotropic compression mechanism was detected. This change is interpreted to result from the appearance of Si_2O_7 dimer defects, as deduced from Raman spectroscopy; the appearance of such defects also accounts for the previously reported pressure-induced amorphization observed for this material upon additional compression. Furthermore, this behavior is followed by a spin crossover of Fe^{2+} that occurs over a wide pressure range, as revealed by Mössbauer spectroscopy.

Introduction

The magnesium–iron silicate mineral olivine, $(\text{Mg}_{1-x}\text{Fe}_x)_2\text{SiO}_4$, with $x \approx 0.1$ – 0.2 is one of the main minerals constituting the Earth's crust and upper mantle,¹ and its high-pressure and high-temperature properties are of great interest for the earth sciences. Olivine forms a solid solution between the two end-members of this mineral series, fayalite (Fe_2SiO_4) and forsterite (Mg_2SiO_4). Mg_2SiO_4 transforms to modified spinel (wadsleyite) and spinel (ringwoodite) structures upon heating at ~ 13.5 and ~ 18 GPa,^{2,3} respectively, while Fe_2SiO_4 directly transforms to the spinel structure at ~ 8 GPa.⁴

In olivine at ambient conditions (orthorhombic, space group $Pbnm$),⁵ Si atoms are coordinated with four O atoms to form $[\text{SiO}_4]$ tetrahedra, while (Mg, Fe) atoms are surrounded by six O atoms. There are two kinds of (Mg, Fe) sites, one on the inversion center and the other on the plane of mirror symmetry (the M1 and M2 sites, respectively).

Application of pressure was reported to induce amorphization at ~ 39 GPa for Fe_2SiO_4 ⁶ and above 70 GPa for Mg_2SiO_4 .⁷ High-pressure energy-dispersive X-ray diffraction experiments have been performed for the entire series of olivine solid solutions ($0 \leq x \leq 1$),⁸ in which a noticeable change in compressibility occurring at higher pressures for Mg- than for Fe-rich olivines (at 42 and 12 GPa for the respective end-members) was characterized. Therefore, there is a need for an extended high-pressure study of the electronic configuration of iron in olivine, as the substitution of magnesium by iron produces a noticeable downshift in the pressure required to induce the change in compressibility despite the fact that the ionic radii are quite similar ($r_{\text{Mg}^{2+}} \approx 72$ pm and $r_{\text{Fe}^{2+}} \approx 78$ pm^{9–11}). Additionally, in a high-pressure Raman spectroscopy study of a single crystal of Mg_2SiO_4 ,¹² the appearance of spectral changes upon compression was associated with the formation of Si–O–Si linkages between adjacent SiO_4 tetrahedra to give Si_2O_7 dimers. These defects,

* To whom correspondence should be addressed. E-mail: jerome@lpmc.univ-montp2.fr.

[†] Universität Bayreuth.

[‡] European Radiation Synchrotron Facility.

[§] Present address: Institut Charles Gerhardt UMR CNRS 5253, Université de Montpellier II Sciences et Techniques du Languedoc, Place E. Bataillon cc 1503, 34095 Montpellier cedex, France.

(1) Ringwood, A. E. *Geochim. Cosmochim. Acta* **1991**, *55*, 2083.
 (2) Ringwood, A. E.; Major, A. *Earth Planet. Sci. Lett.* **1966**, *1*, 241.
 (3) Akimoto, S.; Fujisawa, H. *J. Geophys. Res.* **1968**, *73*, 1467.
 (4) Furnish, M. D.; Bassett, W. A. *J. Geophys. Res.*, *B* **1983**, *88*, 10333.
 (5) Putnis, A. *Introduction to Mineral Sciences*; Cambridge University Press: New York, 1992; Chapter 6.

(6) Williams, Q.; Knittle, E.; Reichlin, R.; Martin, S.; Jeanloz, R. *J. Geophys. Res. [Solid Earth Planets]* **1990**, *95*, 21549.

(7) Guyot, F.; Reynard, B. *Chem. Geol.* **1992**, *96*, 411.

(8) Andrault, D.; Bouhifd, M. A.; Itié, J. P.; Richet, P. *Phys. Chem. Miner.* **1995**, *22*, 99.

(9) Ahrens, L. H. *Geochim. Cosmochim. Acta* **1952**, *2*, 155.

(10) Pauling, L. *The Nature of the Chemical Bond*; Cornell University Press: Ithaca, NY, 1961.

(11) Shannon, R. D. *Acta Crystallogr.* **1976**, *A32*, 751.

(12) Durben, D. J.; McMillan, P. F.; Wolf, G. H. *Am. Mineral.* **1993**, *78*, 1143.

originally observed in the glass form of Mg_2SiO_4 ,^{13–15} were interpreted to be consistent with the initial appearance of local disorder upon compression as a prelude to amorphization of this compound at higher pressures.

In this contribution, an olivine solid solution having $x = 0.1$ was characterized as a function of pressure at room temperature using Raman spectroscopy, X-ray diffraction, and Mössbauer spectroscopy. The goal of this work was to link a structural and vibrational study of olivine with the same composition to a characterization of the electronic configuration of iron as a function of pressure, in an attempt to better understand the origin of the reported change of compressibility⁸ and the additional pressure-induced disorder^{6,7} observed in this material at higher pressures.

Experimental Section

$(\text{Mg}_{1-x}\text{Fe}_x)_2\text{SiO}_4$ ($x = 0.1$) synthetic olivine was prepared by reducing Fe_2O_3 (50% ⁵⁷Fe-enriched Fe_2O_3 and 50% isotopically normal Fe metal) within a SiO_2/MgO mixture at 1100–1200 °C in a CO/CO_2 gas mixture with $\log(f_{\text{O}_2}) = -11.5$ (chemical potential of oxygen) for 24 h. A homogeneous sample was obtained after several steps of grinding and annealing. The sample structure and electronic configuration of olivine were confirmed by analysis using X-ray powder diffraction and Mössbauer spectroscopy. High-pressure experiments were performed using diamond anvil cells (DACs) at room temperature (295 K) with 250 or 300 μm diameter culet anvils. Powdered samples were loaded into a 100–150 μm cylindrical hole drilled into a Re gasket having an initial thickness of 250 μm that was preindented to 30 μm . The samples were loaded under an argon atmosphere to avoid oxidizing conditions, and pressure was measured on the basis of the shifts of the ruby fluorescence lines.¹⁶ No pressure-transmitting medium was used in order to emphasize the pressure-induced local disorder of olivine obtained under nonhydrostatic conditions, as reported by Guyot et al.⁷ Pressure gradients were estimated to be within 10% of the mean reported pressure on the basis of fluorescence measurements on 2–3 ruby crystals placed within the high-pressure compartment.

⁵⁷Fe Mössbauer spectra¹⁷ were recorded at room temperature in transmission mode on a constant-acceleration Mössbauer spectrometer using a nominal 370 MBq, high specific activity ⁵⁷Co source in a 12 μm Rh matrix (point source). The dimensionless effective thickness was estimated to be approximately 20, corresponding to 50 mg of unenriched Fe/cm². Exposure time for each spectrum was typically between 24 and 48 h.

Ambient-temperature Raman spectroscopy experiments were performed using a Jobin Yvon Labram spectrometer with a 632.8 nm He–Ne excitation line and laser output power of 8 mW. The laser beam was focused using a 50 \times objective, resulting in a spot having a diameter of $\sim 5 \mu\text{m}$.

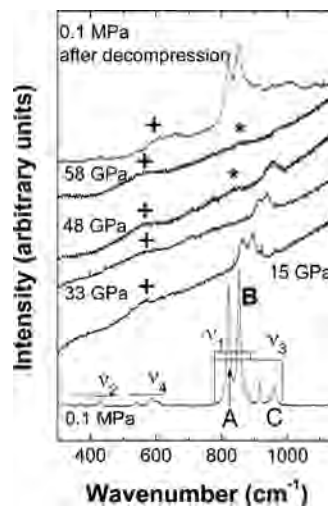


Figure 1. High-pressure Raman spectra of $(\text{Mg}_{0.9}\text{Fe}_{0.1})_2\text{SiO}_4$ at 298 K. The spectrum obtained after decompression is also shown. The internal vibrations of free SiO_4 (ν_1 – ν_4) are indicated along with the strong high-frequency stretching modes of A_g symmetry (A, B, and C). The appearance of a new, very small band (marked with an asterisk) at 48 GPa is associated with Si_2O_7 dimer defects, as proposed by Durben et al.¹² The feature marked with + and the particularly large positively sloped background are due to the fluorescence of diamond from the DAC.

X-ray powder diffraction measurements were performed at the European Radiation Synchrotron Facility (ESRF) on the Swiss-Norwegian Beam Lines (SNBL) using the image plate area detector MAR345. A focused beam having a wavelength of 0.71 Å and a size of 50 $\mu\text{m} \times 50 \mu\text{m}$ was used. The detector-to-sample distance was 319 mm. The collected images were integrated using the Fit2D program¹⁸ in order to obtain a conventional X-ray diagram. An $F(\text{calc})$ weighted fitting procedure was performed using the program GSAS.²² There are three techniques available in GSAS for the extraction of the structure factor from powder data: the “normal” Rietveld method, the Le Bail method, and the $F(\text{calc})$ method using the Pawley technique. The Pawley technique is similar to the Le Bail method, but the values of the reflection structure factors are refined as least-squares variables. These fits were used to obtain accurate unit cell constants; however, because of the low quality of the crystalline data upon (de)compression, no structure analysis was possible. All of the high-pressure X-ray measurements were performed on decompression. X-ray data for the recovered samples were collected with a high-brilliance diffraction system (Rigaku rotating anode, Mo $K\alpha$ radiation) at the Bayerisches Geoinstitut. The X-ray beam was collimated down to a diameter of 50 μm . Diffraction patterns were collected on an APEX CCD detector placed ~ 70 mm from the sample.

Results and Discussion

Raman Spectroscopy Results. High-pressure Raman spectra of $(\text{Mg}_{0.9}\text{Fe}_{0.1})_2\text{SiO}_4$ are shown in Figure 1. In addition to the SiO_4 internal modes,¹⁹ the external Raman modes of olivine are separated into rotatory types for SiO_4 ions and translatory types for SiO_4 ions and for Mg ions at the C_s symmetry sites. Mg ions at the C_i sites do not move during the Raman-active vibration. The Raman spectrum of polycrystalline $(\text{Mg}_{0.9}\text{Fe}_{0.1})_2\text{SiO}_4$ obtained at atmospheric pressure

- (13) Tarte, P. In *Physics of Non-Crystalline Solids*; Prins, J. A., Ed.; Wiley-Interscience: New York, 1965; pp 549–565.
- (14) Lazarev, A. N. *Vibrational Spectra and Structure of Silicates*; Consultants Bureau: New York, 1972.
- (15) Williams, Q.; McMillan, P.; Cooney, T. F. *Phys. Chem. Miner.* **1989**, *16*, 352.
- (16) Mao, H. K.; Xu, J.; Bell, P. M. *J. Geophys. Res. [Solid Earth Planets]* **1986**, *91*, 4673.
- (17) The velocity scale was calibrated relative to 25 μm α -Fe foil using the positions certified for (former) National Bureau of Standards standard reference material no. 1541; line widths of 0.36 mm s^{-1} for the outer lines of α -Fe were obtained at room temperature. Mössbauer spectra were fitted to Lorentzian line shapes using the commercially available fitting program NORMOS, written by R. A. Brand (distributed by Wissenschaftliche Elektronik GmbH, Germany).

- (18) (a) Hammersley, A. P. *ESRF Internal Report*; Report No. ESRF97HA02T; European Synchrotron Radiation Facility: Grenoble, France, 1997. (b) Hammersley, A. P. *ESRF Internal Report*; Report No. ESRF98HA01T; European Synchrotron Radiation Facility: Grenoble, France, 1998.

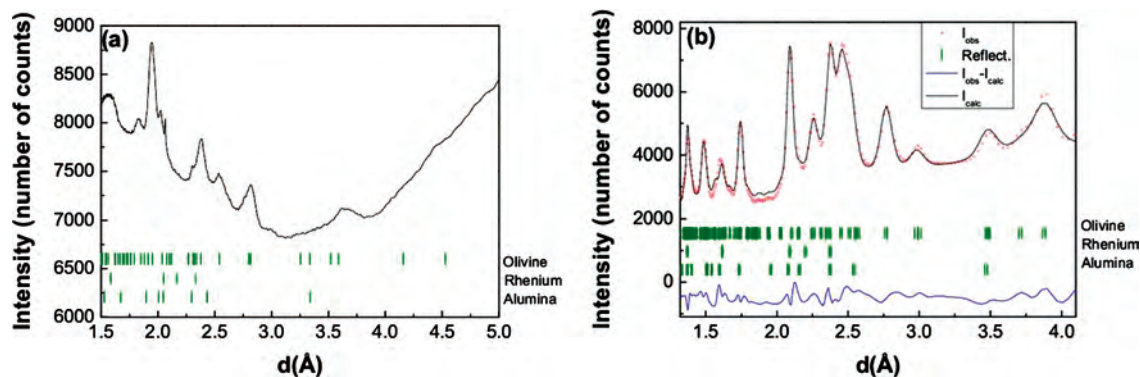


Figure 2. Experimental and calculated profiles of $(\text{Mg}_{0.9}\text{Fe}_{0.1})_2\text{SiO}_4$ obtained during decompression at (a) 45 GPa [fitted using the $F(\text{calc})$ weighted procedure] and (b) atmospheric pressure after decompression [obtained using Rietveld refinement]. Rows of vertical ticks from top to bottom indicate the calculated positions of olivine, rhenium, and alumina from ruby, respectively. In panel (b), the intensity difference (blue trace) is on the same intensity scale.

(Figure 1) is similar to that originally reported²⁰ for an oriented Mg_2SiO_4 single crystal except for the corresponding relative intensities due to the depolarization of the incident and scattered beams in the present case. The internal vibrations of free SiO_4 (ν_1 – ν_4) are indicated along with the strong high-frequency stretching modes of A_g symmetry (A, B, and C), which are due to the crystal-field splitting of the ν_1 and ν_3 modes of free SiO_4 .²¹ On compression, the Raman signal from olivine progressively broadens because of the absence of a pressure-transmitting medium and its associated pressure distribution. At 33 GPa, only the A and B modes can be clearly distinguished, and at 48 GPa, a new, very small broad band (marked with an asterisk) appears at $\sim 840 \text{ cm}^{-1}$. At 58 GPa, only this very small band can be observed, probably because the increased pressure gradient induced a loss of the olivine Raman vibration.

This small bump lies in the frequency range where no Raman scattering occurs in crystalline Mg_2SiO_4 . A similar band has previously been observed (at 720 cm^{-1} under ambient conditions) in glassy Mg_2SiO_4 rapidly cooled to 300 K from temperatures where it is liquid (the melting point of the silicate is as high as 2163 K).^{13–15} Tarte et al.¹³ explained the appearance of this new band in terms of the existence of a fraction of polymerized groups made up of corner-shared SiO_4 tetrahedra (Si_2O_7 dimers).¹³ This particular scattering has also been reported to appear at pressures greater than 30 GPa in a Mg_2SiO_4 single crystal¹² (825 cm^{-1} at 30 GPa, 870 cm^{-1} at 50 GPa) and attributed to the reversible formation of structural defects caused by pressure-induced dimerization of adjacent SiO_4 tetrahedra. These authors further proposed that this could be a precursor to amorphiza-

tion that occurs at higher pressures.⁷ As previously observed by Durben et al.,¹² the recovered sample exhibited the spectral features of olivine with no additional modes but with strain-induced broadening of the Raman line. This suggests that a critical density of defects sufficient to amorphize the olivine could be attained at pressures greater than 58 GPa. The formation of Si_2O_7 dimers obtained by Durben et al.¹² can be associated with the following chemical equation:



The formation of MgO cannot be detected by Raman spectroscopy because this compound has a cubic structure and is therefore inactive on the basis of Raman selection rules.

X-ray Diffraction Results. Diffraction profiles of $(\text{Mg}_{0.9}\text{Fe}_{0.1})_2\text{SiO}_4$ are shown at 45 GPa on decompression (Figure 2a) and 0.1 MPa after decompression from about 70 GPa (Figure 2b). The pattern collected at 45 GPa was fitted using the $F(\text{calc})$ weighted procedure²² in order to obtain unit cell parameters under $Pbnm$ symmetry. The X-ray diffraction data for the sample recovered after decompression were fitted using the Rietveld method. In agreement with the Raman spectroscopy results, the X-ray diffraction pattern of the recovered sample is consistent with the original structure of olivine (space group $Pbnm$). Although the diffraction lines were considerably broadened with pressure, partly as a result of the pressure gradient and the degraded quality of the diffraction data with increasing pressure, no pressure-induced amorphization (which was detected by Raman spectroscopy, as described above) was observed by X-ray diffraction²³ in the investigated pressure range. The volume obtained from fitted unit cell parameters is shown in Figure 3a along with data previously reported for $(\text{Mg}_{1-x}\text{Fe}_x)_2\text{SiO}_4$ ($x = 0, 0.17$) by Andraut et al.⁸ on the basis of energy dispersive X-ray diffraction. Our results are in agreement with their data for pure Mg_2SiO_4 and olivine with $x = 0.17$ (see ref 8 and references therein). Because few pressure points were taken into account, the determination of the bulk modulus is not reliable. A change in

(19) The primitive cell of the end-member Mg_2SiO_4 contains four formula units, leading to the following irreducible representations: $\bar{A} = 11A_g + 11B_g + 7B_{2g} + 7B_{3g} + 10A_u + 10B_{1u} + 14B_{2u} + 14B_{3u}$. Of these, 35 modes are infrared active and 36 modes are Raman active: $11A_g + 11B_g + 7B_{2g} + 7B_{3g}$. One can classify the modes of SiO_4 entities as external or internal and, for the latter, state their derivation. The symmetry of a free SiO_4 ion is T_d , and it has four internal modes of vibration: $\nu_1(A_1)$, $\nu_2(E)$, $\nu_3(F_2)$, and $\nu_4(F_2)$. In Mg_2SiO_4 , however, free SiO_4 ions occupy the C_s symmetry sites, and the anisotropic crystal field in the D_{2h}^6 space group implies a loss of degeneracy for the SiO_4 internal modes.²⁰

(20) Servion, J. L.; Piriou, B. *Phys. Status Solidi B* **1973**, *55*, 677.

(21) Iishi, K. *Am. Mineral.* **1978**, *63*, 1198.

(22) Larson, A. C.; Von Dreele, R. B. *GSAS: General Structure Analysis System*; Los Alamos National Laboratory: Los Alamos, NM, 1994.

(23) For an example of pressure-induced amorphization characterized by X-ray diffraction, see: Swamy, V.; Kuznetsov, A.; Dubrovinsky, L. S.; McMillan, P. F.; Prakapenka, V. B.; Shen, G.; Muddle, B. C. *Phys. Rev. Lett.* **2006**, *96*, 135702.

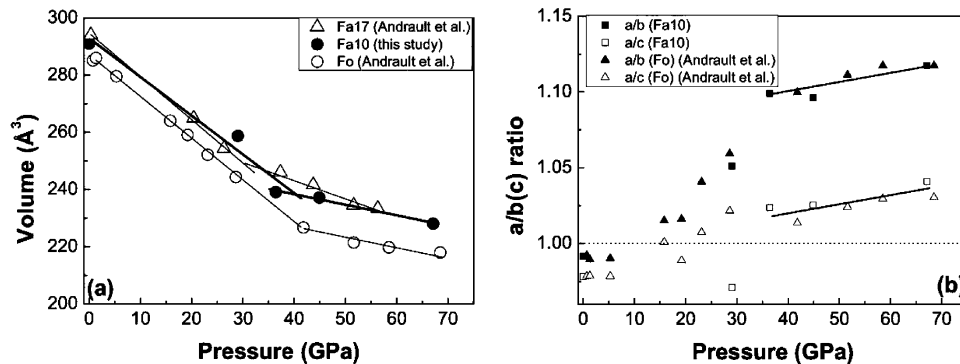


Figure 3. (a) Pressure dependence of the unit cell volume of $(\text{Mg}_{0.9}\text{Fe}_{0.1})_2\text{SiO}_4$ (Fa10, ●) and those reported by Andraut et al.⁸ for $(\text{Mg}_{1-x}\text{Fe}_x)_2\text{SiO}_4$ with $x = 0$ (Fo, ○) and $x = 0.17$ (Fa17, △). (b) Variation with pressure of observed a/b and a/c ratios normalized to the corresponding ratios for an ideal hcp lattice (dotted line) for $(\text{Mg}_{0.9}\text{Fe}_{0.1})_2\text{SiO}_4$ and Mg_2SiO_4 .

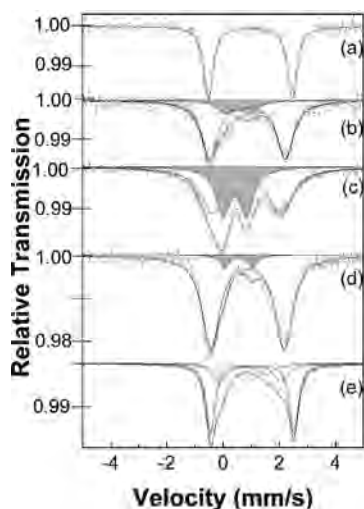


Figure 4. Room-temperature Mössbauer spectra of $(\text{Mg}_{0.9}\text{Fe}_{0.1})_2\text{SiO}_4$ olivine in the DAC at (a) 12 GPa, (b) 52 GPa, (c) 75 GPa, (d) 48 GPa in a second compression, and (e) atmospheric pressure after decompression. Components are shaded as follows: HS Fe^{2+} (unshaded); LS Fe^{2+} (gray). The additional low-intensity spectra in panel (e), which are additional HS components, could be associated with strains induced during (de)compression.

compressibility can be distinguished at ~ 40 GPa. At low pressures, the most compressible direction is along the b axis, in accordance with the data of Andraut et al.⁸ This is consistent with the electronic band structure calculated for fayalite, which shows a relatively large dispersion along the $[010]$ direction that can be compared with the marked flatness along the $[001]$ and $[100]$ directions.^{24,25} The decrease in compressibility observed at ~ 40 GPa originates predominantly from a decrease in compression of the b axis. This change in compressibility can be associated with either a structural phase transition or a change in the electronic configuration of iron (arising from a spin, insulator–metal, or magnetic transition). Since the compressibility change is observed for iron-free olivine, a change in the iron electronic state cannot be the origin of this high-pressure behavior. Thus, we next will discuss the possibility of a structural phase transition in this pressure range.

The anisotropic compression behavior of olivine was previously proposed²⁶ to correspond to a high-pressure

transformation of the oxygen sublattice into an ideal hexagonal close-packed (hcp) lattice. The alb^{27} and alc^{28} ratios of the unit cell of olivine normalized to the corresponding ratios for an ideal hcp lattice are shown in Figure 3b. It is clear that the high-pressure data ($P > 40$ GPa) are not consistent with the geometry of the ideal hcp structure. On the other hand, the alb and alc ratios exhibit almost the same slopes with pressure, indicating a change of the compression behavior of olivine from anisotropic to isotropic. Interestingly, a transformation to the high-pressure, high-temperature spinel structure² (space group $Fd\bar{3}m$) would also result in the same type of behavior, as noted by Kudoh et al.,²⁹ Andraut et al.,⁸ and Durben et al.¹² In this spinel form, O is in a cubic close-packed array with (Mg, Fe) at one-eighth of the tetrahedral sites and Si at half of the octahedral sites. Such a coordination change from 4 to 5–6 for silicon with increasing pressure has previously been observed in high-pressure extended X-ray absorption fine structure spectra on germanate glasses.³⁰ However, there is a large energy barrier (reconstructive phase transition) preventing the transformation to the spinel structure.

On the basis of this analysis of the results displayed in Figure 3b, we propose that the observed anisotropic-to-isotropic change in compressibility more likely corresponds to a saturation of the compressibility mechanism in the olivine structure. When the pressure is increased out of the stability field of the structure, the olivine atomic configurations are “frozen” and an atomic rearrangement is required because of the saturation of the compression mechanism, leading to the appearance of structural defects. These structural defects can be linked to the appearance of Si_2O_7 dimer defects at high pressures ($P > 30$ GPa), as reported by Durben et al.¹² in their Raman spectroscopy study of forsterite.

The change in compressibility observed by Andraut et al.⁸ was also found to take place at higher pressures for Mg than for Fe-rich olivines; the change occurred at 42 and 12 GPa for Mg_2SiO_4 and Fe_2SiO_4 , respectively,⁸ and at ~ 40

(26) Kudoh, Y.; Takeuchi, H. *Z. Kristallogr.* **1985**, *171*, 291.

(27) $[(alb)_{P_{\text{hnm}}}]_{\text{norm}} = (alb)_{P_{\text{hnm}}} / (\sqrt{2/3})$.

(28) $[(alc)_{P_{\text{hnm}}}]_{\text{norm}} = (alc)_{P_{\text{hnm}}} / (2/3)^{1/2}$.

(29) Kudoh, Y.; Takeda, H. *Phys. B* **1986**, *139–140*, 333.

(30) Calas, G.; Brown, G. E.; Farges, F.; Galois, L.; Itié, J. P.; Polian, A. *Nucl. Instrum. Methods Phys. Res., Sect. B* **1995**, *97*, 155.

(24) Cococcioni, M.; Dal Corso, A.; de Gironcoli, S. *Phys. Rev. B* **2003**, *67*, 094106.

(25) Jiang, X.; Guo, G. Y. *Phys. Rev. B* **2004**, *69*, 155108.

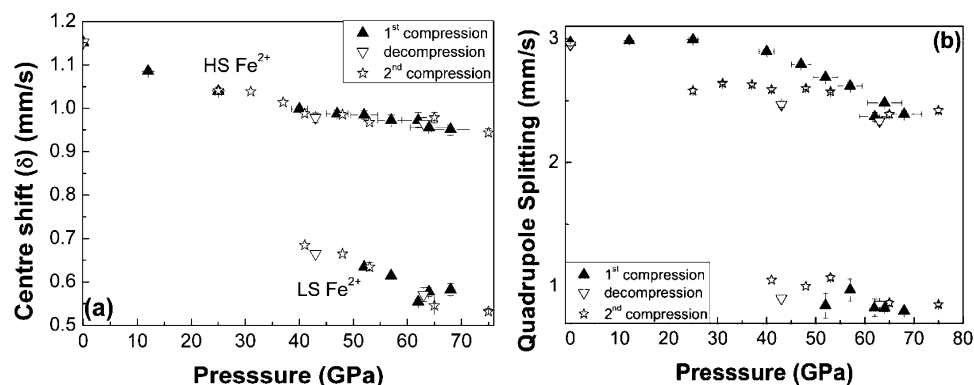


Figure 5. Pressure dependence of (a) the center shift and (b) the quadrupole splitting.

GPa for $(\text{Mg}_{0.9}\text{Fe}_{0.1})_2\text{SiO}_4$ in the present study. We have already mentioned that the compressibility change was a consequence of neither a change in the iron state nor a structural phase transition, but was most probably due to a saturation of the compression mechanism. At the same time, the fact that the substitution of magnesium by iron in the olivine structure implies a downshift in the pressure required for saturation of the compression mechanism (from 42 to 12 GPa) means that the electronic configuration of iron could be implicated in the high-pressure behavior of this solid solution. Therefore, as a complement to the vibrational and structural results discussed above, the findings of our high-pressure Mössbauer study are presented below.

Mössbauer Spectroscopy Results. The pressure dependence of the room-temperature Mössbauer spectrum of $(\text{Mg}_{0.9}\text{Fe}_{0.1})_2\text{SiO}_4$ is shown in Figure 4. The Mössbauer spectra at low pressures show a quadrupole doublet arising from Fe^{2+} at the M1 and M2 sites (Figure 4a). At pressures above 50 GPa, a new component with a significantly smaller center shift (δ) and quadrupole splitting (QS) appears (Figures 4b and 5), whose intensity increases with increasing pressure. It is worth noting that the Mössbauer parameters of this second doublet are not similar to those of the high-pressure, high-temperature spinel form of olivine mentioned above ($\delta = 1.1 \text{ mm/s}$ and $\text{QS} = 2.63 \text{ mm/s}$ at ambient conditions³¹). At higher pressures, this second quadrupole doublet becomes well-resolved, and at 75 GPa (the highest pressure obtained, Figure 4c), the relative area associated with this component reaches $\sim 37\%$. Upon decompression to atmospheric pressure, the new component disappears and the Mössbauer spectrum of the recovered sample is consistent with all of the iron being present as high-spin (HS) Fe^{2+} but existing in a range of different environments (Figure 4e). This behavior is consistent with previously reported⁷ progressive pressure-induced amorphization associated with strains induced during (de)compression. However, even if this process were found to be reversible in this pressure range on the basis of the Raman data (since the recovered sample still exhibited the spectral features of olivine without any additional modes), the broadening of the Raman line obtained after decompression as well as the broadening of olivine diffraction reflections implies the appearance of local dis-

order. This disorder corresponds to a local breakdown of the olivine symmetry, which means that the M1 and M2 sites of iron are randomly shifted from their point symmetry positions; these shifts are manifested in the Mössbauer spectrum of the recovered sample by a distribution of the quadrupole splitting for the M1 and M2 sites.

We propose that the changes in the Mössbauer spectra of olivine $(\text{Mg}_{0.9}\text{Fe}_{0.1})_2\text{SiO}_4$ in the 40–50 GPa pressure range are due to a high-spin to low-spin (HS–LS) transition. The decrease of $\sim 0.25 \text{ mm/s}$ in the center shift in the Mössbauer data is large (Figures 4 and 5a), and a significant electron-density redistribution, such that the s-electron density at the ^{57}Fe nucleus is enhanced by $\Delta\rho(0) \approx 0.8 \text{ au}^{32}$ in the high-pressure phase, is required in order to account for it. The observed change in the center shift is consistent with those previously observed ($0.9\text{--}0.6 \text{ mm s}^{-1}$) for spin-pairing transitions under pressure in various iron–oxygen compounds.^{33,34} Typically, Mössbauer spectra of HS Fe^{2+} show relatively large quadrupole splittings ($\Delta E_Q \approx 2\text{--}3 \text{ mm s}^{-1}$) and isomer shifts ($\delta \approx 1 \text{ mm s}^{-1}$), while for LS Fe^{2+} , these parameters generally have smaller values ($\Delta E_Q \leq 1 \text{ mm s}^{-1}$, $\delta \leq 0.5 \text{ mm s}^{-1}$).³⁵ Additionally, the center shift of the HS and LS components varies consistently with pressure during both compression and decompression (Figure 5a). The relative area of the quadrupole doublet associated with the LS component of olivine is related to its abundance; the pressure dependence of this relative abundance (Figure 6) implies that the spin crossover occurs over a wide pressure range, as previously observed in other iron oxide spin transitions as a function of pressure.³³ A simple linear extrapolation of this data (Figure 6) indicates that 100% transformation is achieved at $\sim 110 \text{ GPa}$.

Finally, the quadrupole splittings of the HS and LS components are consistent with a small hysteresis behavior (Figure 5b). This hysteresis behavior cannot be observed for the center shift, probably as a result of the degraded quality of the Mössbauer data during compression–decompression and the low signal-to-noise ratio. Upon decompression to

(31) Choe, I.; Ingalls, R.; Brown, J. M.; Sato-Sorensen, Y. *Phys. Chem. Miner.* **1992**, *19*, 236.

(32) Ingalls, R.; Van der Woude, A.; Sawatzky, G. A. *Mössbauer Isomer Shifts*; Shenoy, G. K., Wagner, F. E., Eds.; North-Holland: Amsterdam, 1978; Chapter 7.

(33) Kantor, I. Y.; Dubrovinsky, L. S.; McCammon, C. A. *Phys. Rev. B* **2006**, *73*, 100101(R).

(34) Speziale, S.; Milner, A.; Lee, V. E.; Clark, S. M.; Pasternak, M. P.; Jeanloz, R. *Proc. Natl. Acad. Sci. U.S.A.* **2005**, *102*, 17918.

(35) Gülich, P.; Garcia, Y.; Goodwin, H. *Chem. Soc. Rev.* **2000**, *29*, 419.

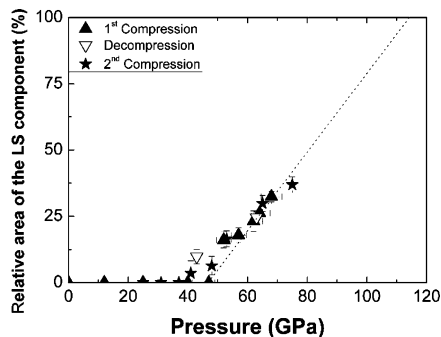


Figure 6. Relative area of the second quadrupole doublet (i.e., the LS component of the Mössbauer spectra) for $(\text{Mg}_{0.9}\text{Fe}_{0.1})_2\text{SiO}_4$ as a function of pressure.

atmospheric pressure, the Mössbauer spectrum of the recovered sample is consistent with all iron being present as HS Fe^{2+} but existing in a range of different environments characterized by a distribution of quadrupole splitting (Figure 4e).

Conclusions

In this study, $(\text{Mg}_{0.9}\text{Fe}_{0.1})_2\text{SiO}_4$ olivine was investigated as a function of pressure using Raman spectroscopy, X-ray diffraction, and Mössbauer spectroscopy. A change in compressibility at ~ 40 GPa was characterized and linked to saturation of the anisotropic compression mechanism of olivine. This change in compressibility is accompanied by the appearance of Si_2O_7 dimer defects, as deduced on the

basis of Raman spectroscopy by Durben et al.¹² However the pressure range investigated under nonhydrostatic conditions was insufficient to reach the critical density of defects needed to cause the olivine structure to become amorphous. A similar change in compressibility was previously observed in $(\text{Mg}_{1-x}\text{Fe}_x)_2\text{SiO}_4$ solid solutions and found to occur at higher pressures for Mg- than for Fe-rich olivines.⁸ High-pressure Mössbauer data obtained at room temperature for $(\text{Mg}_{0.9}\text{Fe}_{0.1})_2\text{SiO}_4$ can be interpreted in terms of a spin transition that occurs over a wide pressure range. The fact that the substitution of magnesium by iron in the olivine structure implies a downshift in the pressure required for saturation of the structural compression mechanism (from 42 to 12 GPa) means that the spin transition of iron could be implicated in the high-pressure behavior of this solid solution. As noted in the Introduction, the ionic radii of magnesium and iron are similar ($r_{\text{Mg}^{2+}} \approx 72$ pm and $r_{\text{Fe}^{2+}} \approx 78$ pm⁹⁻¹¹); however, the spin transition of iron implies a decrease in the iron ionic radius ($r_{\text{Fe}^{2+}(\text{LS})} \approx 61$ pm⁹⁻¹¹). This could result in local collapse of the structure, which could explain the downshift in pressure at which saturation of the olivine structural compression mechanism occurs.

Acknowledgment. This study was supported by the Deutsche Forschungsgemeinschaft (DFG) and the ESF Euro-MinSci program.

IC701983W